

## **Analysis of the torque ripple of permanent magnet synchronous motors with inset and embedded magnets**

**George Todorov**

---

*Analysis of the torque ripple of permanent magnet synchronous motors with inset and embedded magnets (George Todorov). This paper analyzes with magnetic field distribution and torque ripple of Permanent Magnet Synchronous Motors (PMSM) with inset and embedded magnets. An analytical model of the motor has been developed. The model uses iterative procedure and Finite Element Analysis (FEA) to obtain the stator windings flux linkage, direct-axis and quadrature-axis inductances and phase shift between the quantities. Using this model the distribution of the magnetic field produced by the permanent magnets and the magnetic field at operation with rated load have been obtained and shown for both rotor constructions. The torque ripple has been calculated at operation of the motors at rated speed and rated load. It was found that the motor with inset permanent magnets shows smoother operation, while the motor with embedded permanent magnets offers better opportunities for field weakening.*

*Изследване на пулсациите на момента на синхронни двигатели с повърхностно вложени и с вкопани постоянни магнити (Георги Тодоров). В статията се анализира разпределението на магнитното поле и пулсациите на момента на двигатели с повърхностно вложени и с вкопани постоянни магнити. Разработен е аналитичен модел на двигателите. В модела се използва итеративна процедура и анализ с метода на крайните елементи за намирането на потокоспеплението на статорната намотка, индуктивностите по надлъжната и напречната оси и дефазирането между величините. С него е определено разпределението на магнитното поле създадено от постоянните магнити и на магнитното поле при работа на двигателя с номинално натоварване. Изчислени са пулсациите на момента при номинална скорост и натоварване. Резултатите показват, че двигателят с повърхностно вложени магнити има по-плавен характер на изменение на момента, докато двигателят с вкопани магнити е по-подходящ за регулиране на скоростта с отслабване на полето.*

---

### **Introduction**

Permanent magnet synchronous motors (PMSM) have a series of advantages as high efficiency, high torque per volume density and opportunities for precise and wide range speed control. With the increasing energy efficiency requirements, these types of motors are more and more preferred when building energy efficient and precise drives. On other hand this increases the requirements in regards of the stable and noiseless performance of the motor.

PMSM with magnets mounted on the surface of the rotor have a typical non-saliency, just as the non-salient pole electrically excited synchronous motors. The equivalent air-gap is large and circumferentially uniform, which results in a weak armature reaction and equal direct-axis and quadrature-axis

inductances. Rotor configurations with inset and embedded magnets show a clearly defined saliency. The air gap is small and the permeance in the quadrature axis is greater than that in the direct axis. This results in a lower direct-axis inductance compared to the quadrature-axis inductance, unlike the salient pole electrically excited synchronous motors, where  $L_d > L_q$ . Reduced air gap creates preconditions for a stronger manifestation of additional effects disturbing the smooth and steady operation of the motors. Different authors have studied these effects and measures to reduce their impact [1], [2], [3], [4]. The current paper presents an analysis of the torque ripple of PMSM with inset and embedded magnets (Fig. 1b and 1c) in steady state operation at rated load.

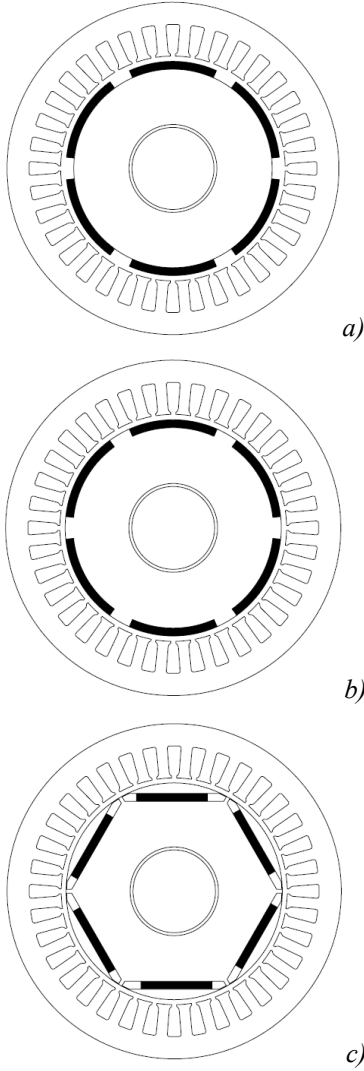


Fig.1. Rotor configurations of PMSM  
a) surface PM; b) inset PM; c) embedded PM.

One reason for the occurrence of torque ripple is the non-sinusoidal distribution of the air gap flux density and the back e.m.f. Stator slot openings and saturation of stator teeth deform the flux density curve and increase the total harmonic distortion [1], [2], [3]. The higher order harmonics of the magnetic flux create additional torques. These additional torques superimpose to the fundamental harmonic torque and result in a torque ripple. The torque ripples are the reason for increased noise and vibrations, which worsen the smooth performance of the motor and the whole drive system.

### Parameters at rated load

To analyze the electromagnetic torque it is necessary to determine the quantities corresponding to the rated load operation of the motor. It is suitable to

develop the model of the motors in a rotor oriented reference frame (d-q reference frame), transforming the real three-phase quantities into two-axes reference frame by using the Park transformation.

The procedure for determining the rated values of the quantities is performed in the following sequence. A preliminary design is done to assign the values for windings wiring data and the cross section geometry [8]. Using this data, a model of the motor is built using FEMM software. The three phase currents are taken for a moment of time where the current in phase A is at the maximum and are assigned to the corresponding windings (with the assumption of sinusoidal distribution):

$$\begin{aligned} i_A &= \sqrt{2} I_1 \cos \omega t \\ (1) \quad i_B &= \sqrt{2} I_1 \cos(\omega t - 120^\circ) \\ i_C &= \sqrt{2} I_1 \cos(\omega t - 240^\circ) \end{aligned}$$

A FEA is performed on the model. The flux linkage of each phase is determined by using the magnetic vector-potential A [5]:

$$(2) \quad \Psi = w_c \cdot \frac{l_m}{S_z} \left( \int_{S_{z+}} A_z dS - \int_{S_{z-}} A_z dS \right)$$

where  $w_c$  is the number of turns in a coil of the phase winding,  $l_m$  is the active length of the coil,  $S_z$  is the cross section of the stator slot occupied by the phase winding,  $A_+$  and  $A_-$  are the values of the vector potential for the positive and negative sides of the coils.

The Park transformation is applied for transforming the three phase quantities into a two axis d-q reference frame fixed to the rotor. The direct-axis and quadrature-axis space vector components of the stator current and flux linkage are determined as:

$$(3) \quad i_d = \frac{2}{3} \left( i_A \cos \theta_r + i_B \cos(\theta_r - \frac{2\pi}{3}) + i_C \cos(\theta_r - \frac{4\pi}{3}) \right)$$

$$(4) \quad i_q = -\frac{2}{3} \left( i_A \sin \theta_r + i_B \sin(\theta_r - \frac{2\pi}{3}) + i_C \sin(\theta_r - \frac{4\pi}{3}) \right)$$

$$(5) \quad \Psi_d = \frac{2}{3} \left( \Psi_A \cos \theta_r + \Psi_B \cos(\theta_r - \frac{2\pi}{3}) + \Psi_C \cos(\theta_r - \frac{4\pi}{3}) \right)$$

$$(6) \quad \Psi_q = -\frac{2}{3} \left( \Psi_A \sin \theta_r + \Psi_B \sin(\theta_r - \frac{2\pi}{3}) + \Psi_C \sin(\theta_r - \frac{4\pi}{3}) \right)$$

where  $\theta_r$  is the rotor position angle (the angle between the d-axis and the magnetic axis of phase A).

The flux linkage  $\Psi_{PM}$  of the stator winding due to the permanent magnets (PM) is determined from the demagnetization curve and the dimensions of the magnets and it is used to calculate the direct-axis and quadrature-axis components of the synchronous inductance and reactance.

$$(7) \quad L_d = \frac{(\Psi_d - \Psi_{PM})}{i_d}$$

$$(8) \quad L_q = \frac{\Psi_q}{i_q}$$

$$(9) \quad x_d = \omega_1 \cdot L_d \quad , \quad x_q = \omega_1 \cdot L_q$$

The determination of the operating point of the motor, corresponding to the rated load, is done by an iterative procedure for defining the numerical values of  $i_d, i_q, L_d, L_q$ , the current phase angle  $\beta$  and the load angle  $\theta$ . The procedure stops when such values are determined, that balance the voltage equation

$$(10) \quad u_s = E_0 + j\omega_1 \cdot L_q \cdot i_q + j\omega_1 \cdot L_d \cdot i_d + R_s \cdot i_s$$

that is graphically depicted in Fig. 2.

The electromagnetic torque of the motor is:

$$(11) \quad T_e = \frac{3}{2} p (\Psi_d \cdot i_q - \Psi_q \cdot i_d)$$

The torque has a constant value when the air-gap is uniform and the distribution of the air-gap flux density is sinusoidal. The slotting of the stator magnetic core makes the circumferentially permeance non-uniform and the saturation of the magnetic circuit deforms the

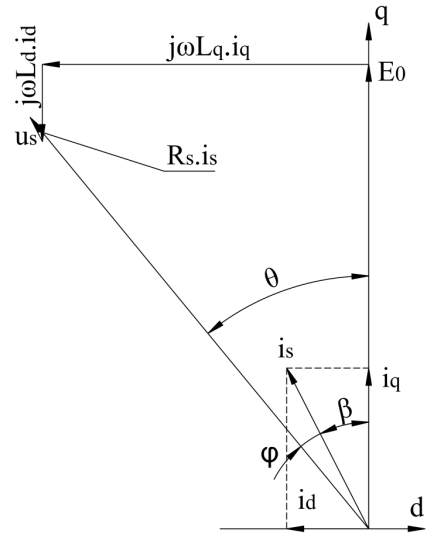


Fig.2. Vector diagram of PMSM motor at rated load.

flux density curve. This causes the occurrence of high order harmonic components of the magnetic induction, the electromotive force and the torque and as a result the torque ripple.

#### Analysis of the torque ripple

To determine the torque ripple, the rotation of the rotor is modeled at rated speed and load. This corresponds to the rotation of the rotor reference frame at an angle  $\theta_r$ , with respect to the stationary stator reference frame – Fig. 3.

The displacement angle between the rotor and stator reference frames is  $\theta_r = \omega_r \cdot t$  (electrical degrees), which corresponds to rotation of the rotor at  $\frac{\theta_r}{p}$  (mechanical degrees). When the rotor rotates with

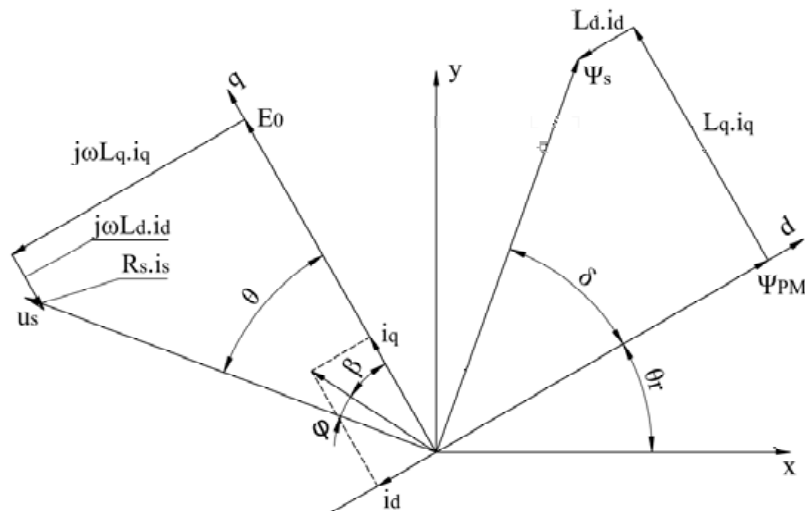


Fig.3. Vector diagram with rotor reference frame at an angle  $\theta_r$ , with respect to the stator reference frame.

angular speed  $\omega_r$ , all vectors depicted in the rotor reference frame rotate at an angle  $\theta_r$  with respect to the stationary stator reference frame.

The analysis of the motors torque ripple is carried out by modeling the rotor rotation with the aid of FEMM software for  $\theta_r = (0 \div 2\pi)$  with a step of 1 electrical degree. A FEA analysis is performed for every angular position to obtain the values of the synchronous inductances by (7) and (8) and torque by (11).

The analysis is illustrated for six-pole PMSM motors with inset and embedded permanent magnets. The rated power of the motors is 2,2 kW and they use equal rated current and thickness of the permanent magnets of 4 mm.

The air-gap flux density distribution for one pole pitch without armature current is shown in Fig. 4.

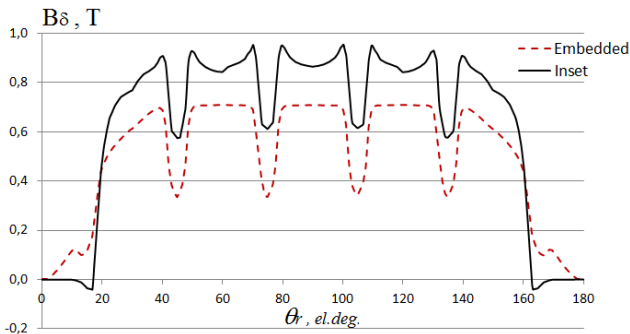


Fig.4. Distribution of the air-gap flux density due to PM.

In the rotor configuration with embedded magnets, the magnets are fully surrounded by ferromagnetic material. This makes possible for a part of the magnet's flux to enclose through the bridge above the magnet and not to cross the air gap. Because of this, the average value of the flux density is much lower than in the case of inset magnets. On other hand, this ferromagnetic bridge increases the permeance of the flux path of the armature reaction and increases the field weakening capabilities of the motor. This is clearly seen from the magnetic flux distribution at rated load of the motor with embedded magnets compared to the motor with inset magnets – Fig. 5 and Fig.6.

The deformation of the flux density distribution caused by the stator slots and the armature reaction leads to an occurrence of high order harmonics. The torques created by these high order harmonics superimpose to the fundamental harmonic torque and result in a torque ripple. The comparison of the torque ripple for the motors under analysis is depicted Fig. 7. It shows that the inset PMSM offers smoother operation at rated speed compared to the motor with embedded magnets.

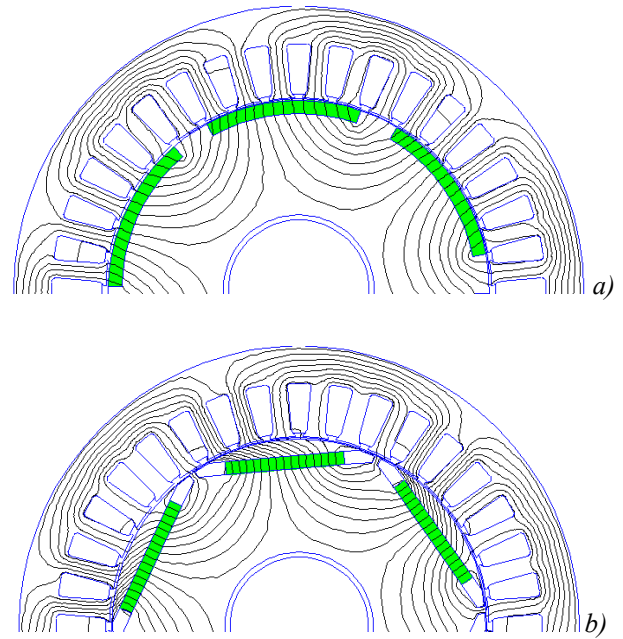


Fig.5. Magnetic flux distribution a) motor with inset PM; b) motor with embedded PM.

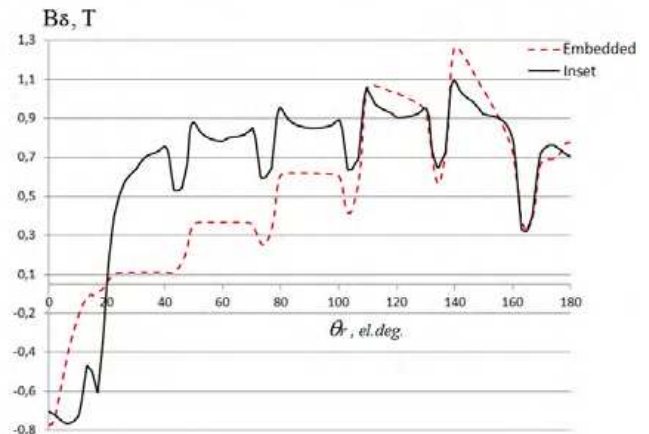


Fig.6. Air-gap flux density distribution for one pole pitch at rated load.

### Conclusion

The torque ripple with high magnitudes and frequency are a reason for noise and vibrations which worsen the performance of the motor and the system it is embedded in. It is of high importance minimizing these ripples at the design stage of the motor. Performing the design using models of the motor that apply FEA combined with the vector diagrams and Park transformations allows the modeling and analysis of different PMSM rotor configurations with required accuracy. The described methods allow the designer to account for unwanted effects such as the torque ripple and to increase the motor performance at the design stage.

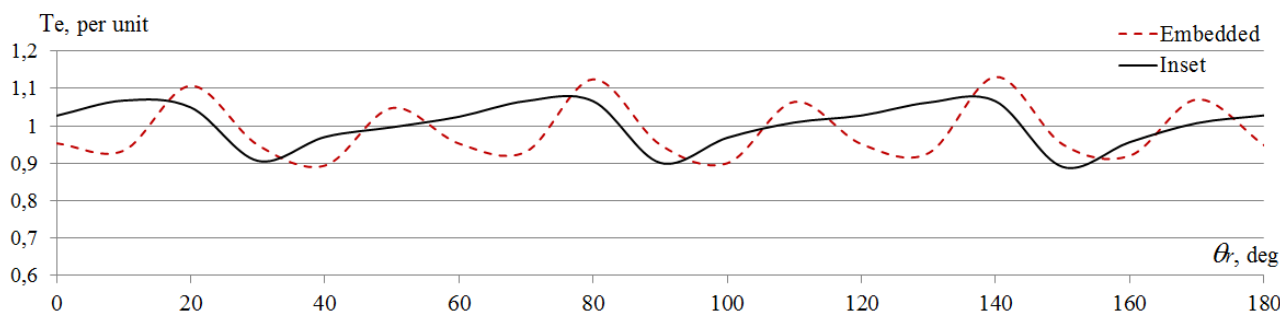


Fig. 7. Torque ripple of the motors with inset and embedded permanent magnets.

Rotor configuration has a great influence on the flux density distribution and therefore on the magnitude and frequency of the ripple. The analysis of the motors with inset and embedded PM shows that the motor with inset magnets demonstrates lower vibrations and a smoother torque.

The configuration with embedded magnets shows torque ripple of greater magnitude which is a premise for increased noise and vibrations. Precautions have to be taken for minimizing the ripple, such as skewing the stator slots or magnets, design the rotor poles with ununiformed air-gap or using ferromagnetic wedges for the stator slots. The armature reaction of this configuration has a greater demagnetizing effect and makes these types of motors suitable for applications where a wide range field-weakening speed control is required.

## REFERENCES

- [1] Chang-Hyun Cho, Chang-Sung Jin. A comparative analysis of two kinds of poles for washing machines PMSM with the same torque and output power. International Conference on Electrical Machines and Systems ICEM 2008, Wuhan, China, 17-20 Oct. 2008, pp. 3099-3101.
- [2] Islam, R., I. Husain. Permanent magnet synchronous motor magnet design with skewing for torque ripple and cogging torque reduction. IEEE Transactions on Industry Applications, Vol. 45, No. 1, January/February 2009, pp. 1552-1559.
- [3] Seok-Hee Han, T.M. Jahns. Torque ripple reduction in interior permanent magnet synchronous machines using the principle of mutual harmonic exclusion. Conference Record of the 2007 IEEE Industry Applications Conference, 23-27 Sept. 2007, pp. 558-565.
- [4] Monteiro, J.R.B.A., A.A. Oliveira Jr. Electromagnetic torque ripple and copper losses reduction in permanent magnet synchronous machines. European Transactions on Electrical Power, Published online in Wiley Online Library ([wileyonlinelibrary.com](http://wileyonlinelibrary.com)).
- [5] Rizov, P., R. Spasov, T. Stoyanov, V. Zahariev. Determining the dependency of the flux linkage from the load in synchronous machines with permanent magnets for hybrid automobiles. Proceedings of the Technical University of Sofia, v. 64, book 4, 2014, pp. 97-104 (in Bulgarian).
- [6] Pyrhonen, J., T. Jokinen, V. Hrabovcová. Design of Rotating Electrical Machines. John Wiley & Sons, Ltd., 2014.
- [7] Chunting Mi, M. Filippa. Analytical Method for Predicting the Air-Gap Flux of Interior-Type Permanent-Magnet Machines. IEEE Transactions on Magnetics, Vol. 40, No. 1, January 2004, pp. 50-58.
- [8] Todorov, G., B. Stoev. Analytical Model for Sizing the Magnets of Permanent Magnet Synchronous Machines. Proceedings of the 14-th International Conference on Electrical Machines, Drives and Power Systems ELMA 2015, Oct. 2015, Varna, Bulgaria, pp. 26-33.

---

**George Todorov, PhD**, graduated and received his PhD degree from the Technical University of Sofia-Bulgaria. His current position is Associate Professor at the Department of Electrical Machines in the Faculty of Electrical Engineering. His research topics are design, analysis, monitoring and diagnosis of electrical machines.

tel.: +359 2 965 2143, e-mail: [gtto@tu-sofia.bg](mailto:gtto@tu-sofia.bg)

**Received on: 23.11.2015**